Rare Metal Materials and Engineering
Volume 53, Issue 3, March 2024
Available online at www.rmme.ac.cn

Science Press

Cite this article as: Lian Xinli, Zhou Jianjun, Li Shilin, et al. Enhancement of Magnetic Properties and Corrosion Resistance for Misch Metal Based RE-Fe-B Magnets Prepared by Double Main Phase Process[J]. Rare Metal Materials and Engineering, 2024, 53(03): 660-666. DOI: 10.12442/j.issn.1002-185X.20230230.

ARTICLE

Enhancement of Magnetic Properties and Corrosion Resistance for Misch Metal Based RE-Fe-B Magnets Prepared by Double Main Phase Process

Lian Xinli[1], Zhou Jianjun[1,3], Li Shilin[1], Zhao Yuanhong[1], Wang Changpeng[1], Wang Yin[1], Liu Fei[1], Zhang Ming[1], Zuo Jianhua[1], Bai Suo[1], Liu Yanli[1], Li Zhubai[2], Li Yongfeng[1]

[1] School of Science, Inner Mongolia University of Science and Technology, Baotou 014010, China; [2] School of Materials and Metallurgy, Inner Mongolia University of Science and Technology, Baotou 014010, China; [3] Ganjiang Innovation Academy, Chinese Academy of Sciences, Ganzhou 341119, China

Abstract: In order to reduce the RE-Fe-B material cost and to balance the utilization of rare earth sources, $[(Pr, Nd)_{1-x}MM_x]_{30.3}(Fe, Co)_{bal}$-$M_{0.73}B_{0.98}$ (x =0.3, 0.5, 0.7, wt%) magnets were prepared by double main phase (DMP) and single main phase (SMP) processes. DMP magnets are superior to SMP magnets with the same nominal composition in magnetic properties and corrosion resistance. For x=0.5, the magnetic properties of DMP magnets are B_r=1.308 T, H_{cj}=799.980 kA/m and $(BH)_{max}$=325.6436 kJ/m^3, which are higher than those for SMP magnets (B_r=1.297 T, H_{cj}=746.8868 kA/m and $(BH)_{max}$=317.8428 kJ/m^3) with the same nominal composition, and the improved RE-rich phase distribution and REs heterogeneity distribution are the main reasons. When DMP magnets are exposed to a hygrothermal environment, there is not only RE-rich phase corrosion, but also pulverized main phase grain due to hydrogenation behavior difference between LaCe-rich and LaCe-lean shell-core within one individual grain. As a result, it is demonstrated that DMP technique is an effective approach to improve the permanent magnetic properties and corrosion resistance of MM-based sintered magnets.

Key words: misch metal; double main phase process; magnetic properties; corrosion resistance; heterogeneous distribution of rare earth

The demands for Nd-Fe-B sintered magnets have been increased in sensors, hybrid vehicles, magnetoelectric machines, etc, due to superior magnetic properties, since they were invented[1–3]. As a result, the closely relied Nd, Pr, Dy and Tb metals are in short supply and high cost, but the relatively highly abundant La and Ce are overstocked commodities and cheap. Hence, La or Ce substitution for Nd to fabricate RE-Fe-B (RE represents rare earth) has become research focus to achieve balanced and high-efficiency application of RE resources[4–7]. Whereas extraction and purification processes for these elements are harmful to the ecological environment. So misch metal (MM) without separation which is composed of 26wt%–29wt% La, 49wt%–53wt% Ce, 4wt%–6wt% Pr and 15wt%–17wt% Nd from Bayan Obo mine is directly applied in RE-Fe-B magnets preparation[6].

However, due to the inferior intrinsic magnetic properties of $La_2Fe_{14}B$/$Ce_2Fe_{14}B$ to those of $Nd_2Fe_{14}B$[8–9], the RE-Fe-B magnets with direct La/Ce/MM substitution prepared by single main phase (SMP) process have more severely deteriorative magnetic properties than Nd-Fe-B magnets[10–13]. To further improve the magnetic properties, the double main phase (DMP) process (blending free-La/Ce/MM and contained-La/Ce/MM powders and sintering) has been employed recently[14–17]. As a result, B_r=1.24 T, H_{cj}=716.4 kA/m, and $(BH)_{max}$=292.132 kJ/m^3 of the DMP magnets with 45wt% Ce substitution were obtained[18]. Subsequently, the DMP magnets with 18wt% La-Ce substitution were successfully

Received date: April 21, 2023
Foundation item: National Key Research and Development Program of China (2022YFB3505800); Natural Science Foundation of Inner Mongolia (2022LH MS05006)
Corresponding author: Liu Yanli, Ph. D., Lecturer, School of Science, Inner Mongolia University of Science and Technology, Baotou 014010, P. R. China, Tel: 0086-472-5954358, E-mail: 2020023217@stu.imust.edu.cn

fabricated by Jin et al[19], whose magnetic properties are B_r= 1.291 T, H_{cj} of 1034.8 kA/m and $(BH)_{max}$=327.952 kJ/m^3. Moreover, the magnets containing 30.3at% MM were prepared by DMP process, and the magnetic properties of them remain H_{cj} =565.956 kA/m and $(BH)_{max}$=326.36 kJ/m^3 [20]. In addition, for DMP magnet with MM/RE=50%, the magnetic performance enhancement was also achieved (B_r=1.278 T, H_{cj}= 658.0532 kA/m and $(BH)_{max}$=289.9032 kJ/m^3), compared with those of SMP magnets (B_r=1.245 T, H_{cj}=358.8368 kA/m and $(BH)_{max}$=242.2228 kJ/m^3) with the same nominal composition[21]. The superior magnetic properties of DMP magnets to those of SMP ones are attributed to the heterogeneous RE distribution within a 2: 14: 1 main phase grain and between grains, as well as the evolution of grain boundary phase[22].

Besides the magnetic properties, the corrosion resistance of magnets containing La/Ce/MM is another critical concern for their application in hot/humid environments. As reported, Nd-La-Ce-Fe-B/Nd-Ce-Fe-B DMP sintered magnets are similar to Nd-Fe-B SMP magnets, which possess 2: 14: 1 matrix phase and RE-rich intergranular phase[23]. In hot/humid environments, for Nd-Fe-B magnets, the RE-rich intergranular phase with relatively lower electrode potential compared with that of the $RE_2Fe_{14}B$ phase acts as the anode in electrochemical reaction[24–26] and is corroded preferentially, and then the $RE_2Fe_{14}B$ phase grains get loose and shed from bulk magnet[27–28]. Therefore, the microstructure and distribution of RE-rich phase play a key role in corrosion resistance. In recent literatures, the DMP magnets containing Ce/La-Ce, with the same nominal composition as SMP magnets exhibit better corrosion resistance as a result of enhanced densification and RE-rich phase distribution[29–33]. Besides, Jin et al[30,34] found that $CeFe_2$ phase in the triple junctions of matrix phase grains has higher electrode potential than the conventional RE-rich phase and can hinder the corrosion channel in DMP magnet containing La-Ce/Ce. When the ratio of Ce/RE exceeds 30wt% in DMP magnets, the $RE_2Fe_{14}B$ matrix phase acts as anode but the RE-rich phase acts as a cathode. So the $RE_2Fe_{14}B$ phase is preferentially corroded, which was revealed by Shi et al[35]. In our previous research, when MM/RE increases from 0wt% to 50wt%, the MM-based magnets prepared by DMP process exhibit higher electrode potential than by SMP method[36]. In order to further reveal the origin of Nd-MM-Fe-B corrosion behavior, comparative studies for DMP and SMP magnets were performed. The accelerated corrosion and electrochemical performance as well as the corroded morphology and corrosion products would also be investigated.

1 Experiment

The casting strips with a nominal composition of $[(Pr, Nd)_{1-x}MM_x]_{30.3}(Fe, Co)_{bal}M_{0.73}B_{0.98}$ (x=0, 0.3, 0.5, 0.7, 1.0, wt%) were prepared by the induction melting and strip casting under high purity argon atmosphere, where M refers to Cu, Al, Co, Ga, and Nb elements. The selected raw material purity was >99.5wt%, and MM was one of the misch metals from the Bayan Obo mine in Baotou, whose composition was 28.63wt% La, 50.13wt% Ce, 4.81wt% Pr, 16.28wt% Nd and balance <1wt%. Subsequently, the alloy strips were ground to the powders by hydrogen decrepitation and jet milling successively. The mean particle size of the obtained fine powder was 3.0–3.5 μm. Afterward, according to the preset nominal composition, part of $(Pr, Nd)_{30.3}(Fe, Co)_{bal}M_{0.73}B_{0.98}$ and $(MM)_{30.3}(Fe, Co)_{bal}M_{0.73}B_{0.98}$ powders were blended to fabricate DMP magnets. The others were used to prepare SMP magnets. Then, the green powders were aligned and compacted under a 2.5 T magnetic field and ~10 MPa pressure, followed by isostatic compressing under 200 MPa. And then sintering (1020–1060 °C for 2 h) and two-stage annealing (900 °C for 2 h and 450–500 °C for 2 h) were applied to obtain DMP and SMP magnets.

The magnetic properties of DMP and SMP magnets were tested by NIM-200C hysteresis graph. To obtain corrosion resistance of both types of magnets, accelerated corrosion tests were performed by placing the columned samples (Φ10 mm×5 mm) under 120 °C, 2×10^5 Pa and 100% relative humidity atmosphere for 24, 48, 72 and 96 h. And the phase constitution of corrosion products was identified by X-ray diffraction (Cu Kα radiation). The surface morphology was observed by a scanning electron microscope (QUANTA 400) after highly accelerated corrosion. The elemental composition of the corrosion was obtained by energy dispersive X-ray spectrometer (EDS). The polarization curves were measured by a VersaSTAT3 electrochemistry analyzer at 25±1 °C in 3.5wt% NaCl solution in a standard three-electrode cell consisting of Nd-Fe-B working electrode, saturated calomel reference electrode and Pt counter electrode.

2 Results and Discussion

Fig. 1 shows the demagnetization curves of $[(Pr, Nd)_{1-x}MM_x]_{30.3}(Fe, Co)_{bal}M_{0.73}B_{0.98}$ (x=0, 0.3, 0.5, 0.7, 1.0) magnets prepared by SMP and DMP processes at 20 °C. Apparently, B_r, H_{cj}, and $(BH)_{max}$ of the prepared magnets by either SMP or DMP process gradually decrease with increasing MM content. However, the magnetic properties of DMP magnets are obviously superior to those of SMP magnets. For instance, compared with MM-free magnets (B_r=1.412T, H_{cj}=1345.24

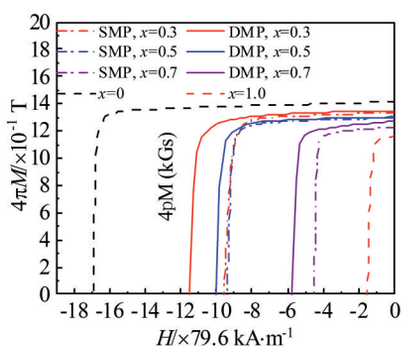

Fig.1 Demagnetization curves of $[(Pr, Nd)_{1-x}MM_x]_{30.3}(Fe, Co)_{bal}M_{0.73}B_{0.98}$ magnets prepared by SMP and DMP processes at 20 °C

kA/m and $(BH)_{max}$=387.0948 kJ/m^3), the magnetic performance of x=0.3 DMP magnets declines to B_r=1.349 T, H_{cj}=917.788 kA/m and $(BH)_{max}$=348.5684 kJ/m^3, but the magnetic properties of x=0.3 SMP magnets deteriorate to B_r= 1.338 T, H_{cj}=756.4388 kA/m and $(BH)_{max}$=338.3796 kJ/m^3. In addition, B_r gradually decreases to 1.238 T by 12.32% but H_{cj} sharply reduces to 459.1328 kA/m by 65.87% with increasing MM content to x=0.7 for DMP magnets. However, for x= 0.5 DMP magnets, the magnetic properties remain B_r=1.308 T, H_{cj} =799.98 kA/m and $(BH)_{max}$=325.6436 kJ/m^3, which are higher than those for SMP magnets (B_r=1.297 T, H_{cj}=746.8868 kA/m and $(BH)_{max}$=317.8428 kJ/m^3) with the same nominal composition. Therefore, the magnetic performance enhancement is not only a result of the inferior intrinsic magnetic properties but also may be related to microstructure, as exhibited by the improving properties of DMP magnets compared with those of SMP magnets.

Fig.2 shows the SEM back-scattered electron (BSE) images for SMP and DMP $[(Pr, Nd)_{1-x}MM_x]_{30.3}(Fe, Co)_{bal}M_{0.73}B_{0.98}$. Similar to conventional Nd-Fe-B, there is a grey $RE_2Fe_{14}B$ matrix phase containing La, Ce, Pr, Nd and a bright RE-rich intergranular phase. Compared with the SMP magnets, in DMP magnets with the same nominal composition, the RE-rich grain boundary layer between adjacent grains is more continuous, which plays a critical role in reducing exchange coupling between grains and enhancing the coercivity effectively.

Besides this, in DMP magnets, there are much less RE-rich phase aggregations in triple junctions of the main phase grains, where reversal domains are prone to nucleate as a result of increased demagnetization filed, compared with the case in SMP magnet. Therefore, DMP magnets have higher coercivity than SMP magnets with the same composition. Furthermore, with increasing MM substitution, RE-rich phase agglomeration regions also increase as a result of La/Ce element from MM aggregating in triple junctions of main grains, which results in decreased coercivity with increasing MM in the both types of magnets. In the corrosion environment, RE-rich phase in the triple junctions is apt to be preferentially corroded on account of high electrodynamic potential and large exposure area, and subsequently corrosion channel is opened. So RE-rich phase agglomeration is harmful to corrosion resistance.

In addition, the RE distributions for DMP magnets are also researched, SEM BSE images for the DMP $[(Pr, Nd)_{0.5}$-$MM_{0.5}]_{30.3}(Fe, Co)_{bal}M_{0.73}B_{0.98}$ magnets and corresponding mappings of La, Ce, Pr, Nd and Fe elements are displayed in Fig. 3. The dark gray regions are $RE_2Fe_{14}B$ matrix phases, and bright regions correspond to RE-rich intergranular phases. Based on the La, Ce, Pr and Nd distributions in Fig. 2, there are inhomogeneous La/Ce/Pr/Nd distributions for x=0.5 DMP magnet. For grain 1, La and Ce are enriched in the center of the main phase grain, but Nd is enriched in the shell region. In contrast, for grain 2, Nd is concentrated in the core region surrounded by the thin La/Ce-rich shell. Further in the regions 3 and 4 in Fig. 3a, there are also inhomogeneous La/Ce/Pr/Nd distribution. In a word, due to diffusion during sintering and annealing processes, heterogeneous REs distributions both within one individual grain and across grains are formed. The heterogeneous REs distributions make exchange coupling in the interior of the matrix grains enhanced[8]. It is beneficial to obtain higher remanence and coercivity for DMP magnets than for SMP magnets.

Due to core-shell structure[37] in grain 1 (Fig. 3) in DMP magnets, elements Pr and Nd with lower chemical activity than La and Ce in the shell regions protect the cores. It is beneficial to improve corrosion resistance.

Fig. 4a shows the potentiodynamic polarization curves for

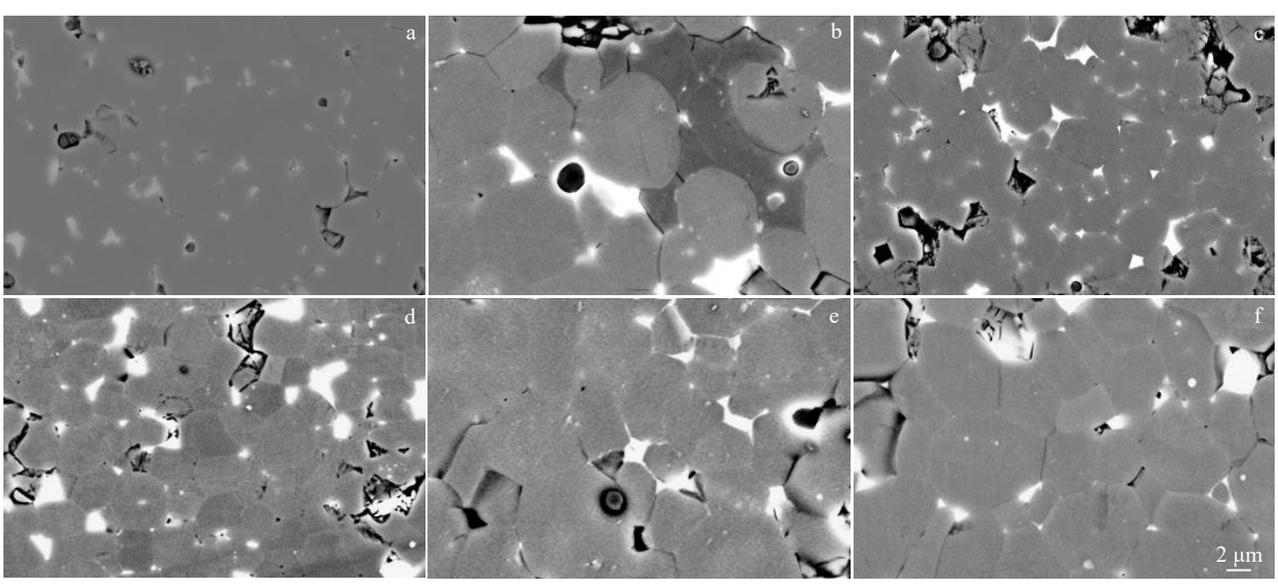

Fig.2 SEM BSE images for $[(Pr, Nd)_{1-x}MM_x]_{30.3}(Fe, Co)_{bal}M_{0.73}B_{0.98}$ magnets prepared by SMP (a–c) and DMP (d–f) processes: (a, d) x=0.3, (b, e) x=0.5, and (c, f) x = 0.7

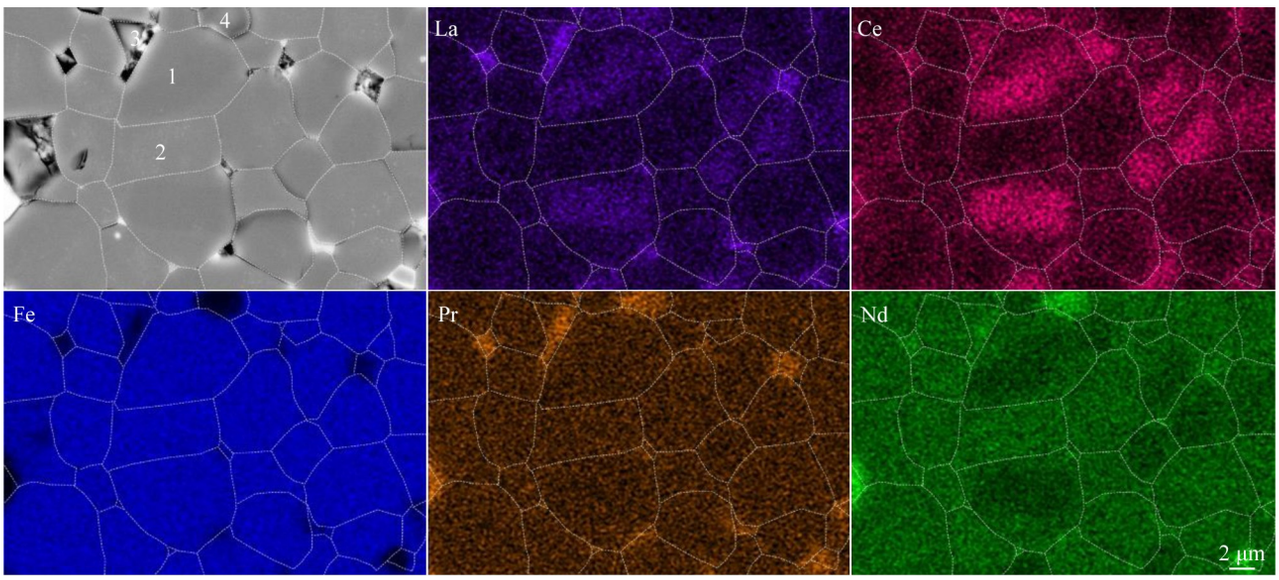

Fig.3 Typical SEM BSE image of DMP $[(Pr, Nd)_{0.5}MM_{0.5}]_{30.3}(Fe, Co)_{bal}M_{0.73}B_{0.98}$ magnets and corresponding EDS mappings of La, Ce, Pr, Nd and Fe elements

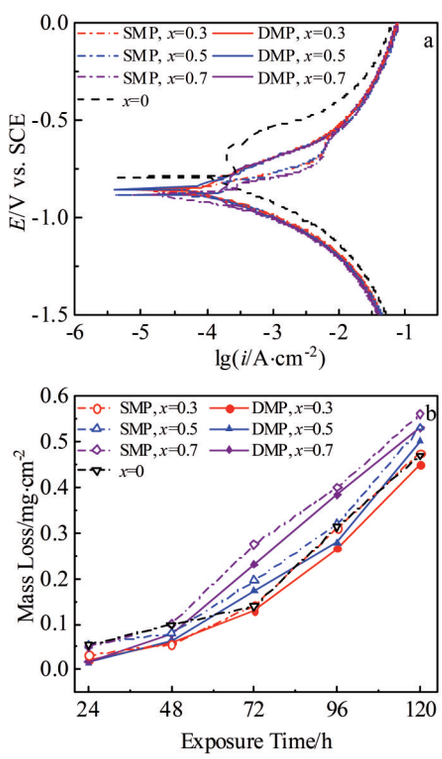

Fig.4 Potentiodynamic polarization curves in 3.5wt% NaCl aqueous solutions (a) and mass loss versus exposure time (b) for $[(Pr, Nd)_{1-x}MM_x]30.3(Fe, Co)_{bal}M_{0.73}B_{0.98}$ magnets prepared by SMP and DMP processes under conditions of 120 °C, 0.2 MPa and 100% relative humid atmosphere

the $[(Pr, Nd)_{1-x}MM_x]_{30.3}(Fe, Co)_{bal}M_{0.73}B_{0.98}$ magnets prepared by SMP and DMP processes in 3.5wt% NaCl aqueous solutions. Their corrosion potential E_{corr} and corrosion current density I_{corr} obtained by the Tafel extrapolation method are summarized in Table 1. Both types of magnets prepared by SMP and DMP processes exhibit a more negative E_{corr} and much higher I_{corr} compared with MM-free magnets and their absolute values get larger with increasing MM content, which implies worse corrosion resistance from the view of thermodynamics. It is attributed to the lower standard electrode potential of LaCe-rich phase ($La \rightarrow La^{3+}+3e^-$, –2.52 V vs. SHE; $Ce \rightarrow Ce^{3+}+3e^-$, –2.48 V vs. SHE) compared with Nd ($Nd \rightarrow Nd^{3+}+3e^-$, –2.25 V vs. SHE)[30], which not only decreases the potential of the LaCe-containing RE-rich phase but also increases the corrosion activity. However, the corrosion potential $|E_{corr}|$ and corrosion current density I_{corr} for DMP magnets are smaller than those for SMP magnets with the same composition. For example, $|E_{corr}|$ =0.887 V and I_{corr}= 1933.3 μA/cm^2 for x=0.7 DMP magnet, but $|E_{corr}|$=0.900 V and I_{corr}=2846.7 μA/cm^2 for x=0.7 SMP magnet. It is further confirmed that DMP magnets are more apt to corrosion resistance. It can be explained by the fact that enhanced RE-rich phase distribution decreases corrosion channel corresponding to triple junctions of the main phase grains. Whereafter, the curves of mass loss versus exposure time for

Table 1 Corrosion potential E_{corr} and corrosion current density I_{corr} for $[(Pr, Nd)_{1-x}MM_x]_{30.3}(Fe, Co)_{bal}M_{0.73}B_{0.98}$ magnets pre-pared by SMP and DMP processes in 3.5wt% NaCl aqueous solutions

x	SMP		DMP	
	E_{corr}/V	I_{corr}/μA·cm^{-2}	E_{corr}/V	I_{corr}/μA·cm^{-2}
0	–0.797	972.16	-	-
0.3	–0.859	2800.9	–0.847	952.41
0.5	–0.871	3350.4	–0.867	1312.7
0.7	–0.900	2846.7	–0.887	1933.3

SMP and DMP containing MM magnets under 120 °C, 0.2 MPa and 100% relative humidity atmosphere are plotted in Fig.4b. The black dotted line represents the mass loss of MM-free magnets in a hot/humid atmosphere as a function of exposure time, but the solid lines and dash-dot lines are corresponding to the mass loss of SMP and DMP magnets, respectively. After exposure for 48–96 h, the DMP magnets show relatively lower mass loss than SMP magnets with the same composition. For comparison, the mass loss values of SMP and DMP magnets with x=0.5 are 0.196 and 0.172 mg/cm^2 after exposure for 72 h under a hot/humid atmosphere, respectively. It may be contributed to the fact that less RE-rich phase aggregations in DMP magnets relative to SMP deplete corrosion channels. And since La/Ce is likely to react with oxygen and vapor, the mass loss rate gradually increases with increasing incremental MM (La and Ce) content and prolonging exposure time.

The corrosion resistance of DMP magnets is superior to that of SMP magnets. For x=0.5 with exposing time of 24 h, part of the RE-rich intergranular phase is preferentially corroded, which makes the polygon mesh-like surface and some clusters of powdery corrosion aggregates (the red dotted region in Fig.5a) emerge for the SMP magnets.

With prolonging exposure time to 120 h, the water vapor infiltrates into the cracks and cavities from the deciduous corroded RE-rich phase, leading to subsequent breakdown of adjacent main phase grains and extensive detachment from the bulk magnet, as shown by the blue circle region in Fig. 5b. In addition, the powdery corrosives get also widely increasing. The evolution is identical to the conventional Nd-Fe-B. However, compared with the SMP magnet, at early 24 h, there is only a small amount of powder from the corrosive RE-rich intergranular phase on the surface of the DMP magnet, but the bulk RE-rich aggregates are also gradually shed from junctions of main phase grains. When the exposure time is prolonged to 120 h, there are some cracks in a fraction of the main phase grains, and there are no large areas of grain shedding. The distinctive corrosion behavior of the SMP magnet may be related to the potential and corrosion activity difference aroused by heterogeneous REs distribution within the main phase grain[34]. Within a grain, the reaction rate of the LaCe-rich shell (core) with vapor is faster than that of the LaCe-lean core (shell), so the shear stress difference between these regions leads to fracture into powders. Therefore, in some main phase grains, there is pitting corrosion.

Fig.6 shows the surface morphologies, line scan results, and XRD patterns for x=0.3 SMP and DMP magnets exposed at 120 °C for 72 h under 0.2 MPa and 100% relative humid atmosphere. In early 72 h under humid air, SMP magnet is similar to conventional Nd-Fe-B. RE-rich phase with relatively higher electrodynamic potential compared with $RE_2Fe_{14}B$ phase reacts preferentially with oxygen and vapor, as confirmed by elemental line scan results in Fig.6e, because there are enriched Pr, Nd, La and Ce but few Fe for corrosion products. Moreover, the corrosion products are mainly $RE(OH)_3$ and RE_2O_3 as identified by XRD patterns in Fig.6f. In humid air and high-temperature atmosphere, due to galvanic corrosion occurring between the RE-rich phase and vapor, $RE(OH)_3$ and hydrogen are formed[38], further leading to hydriding of the RE-rich phase to form a powder, finally causing $RE_2Fe_{14}B$ grains shedding from bulk magnets (the high intensity of XRD patterns besides (001) for the cross section vertical to c-axis in Fig.6f). However, for x=0.3 DMP magnet, under a hygrothermal environment, due to hydrogen formation from chemical reaction among the RE-rich phase,

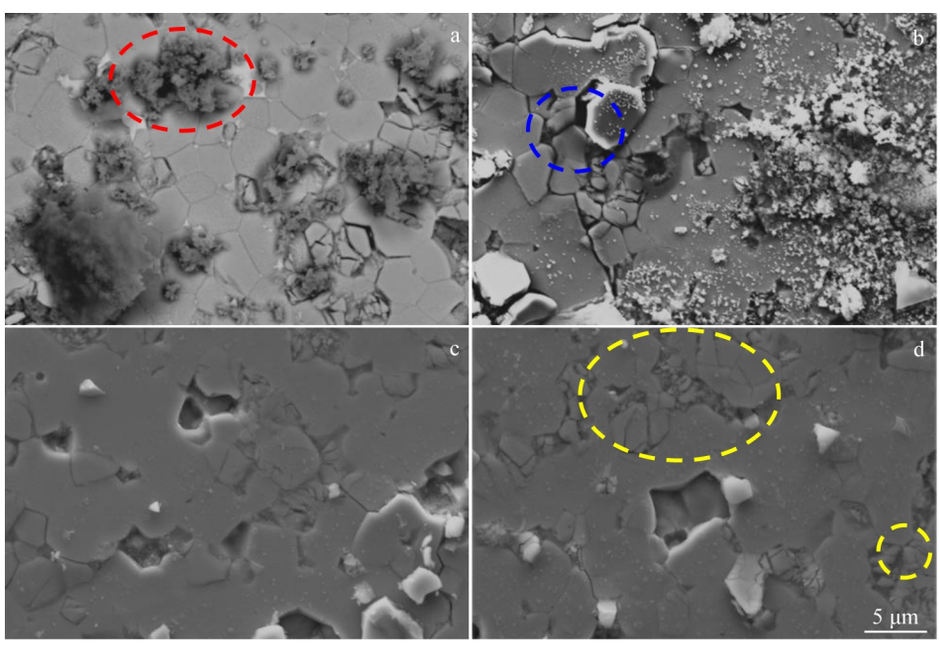

Fig.5 Morphologies for SMP magnets with exposing time of 24 h (a) and 120 h (b) under 120 °C, 0.2 MPa and 100% relative humid atmosphere

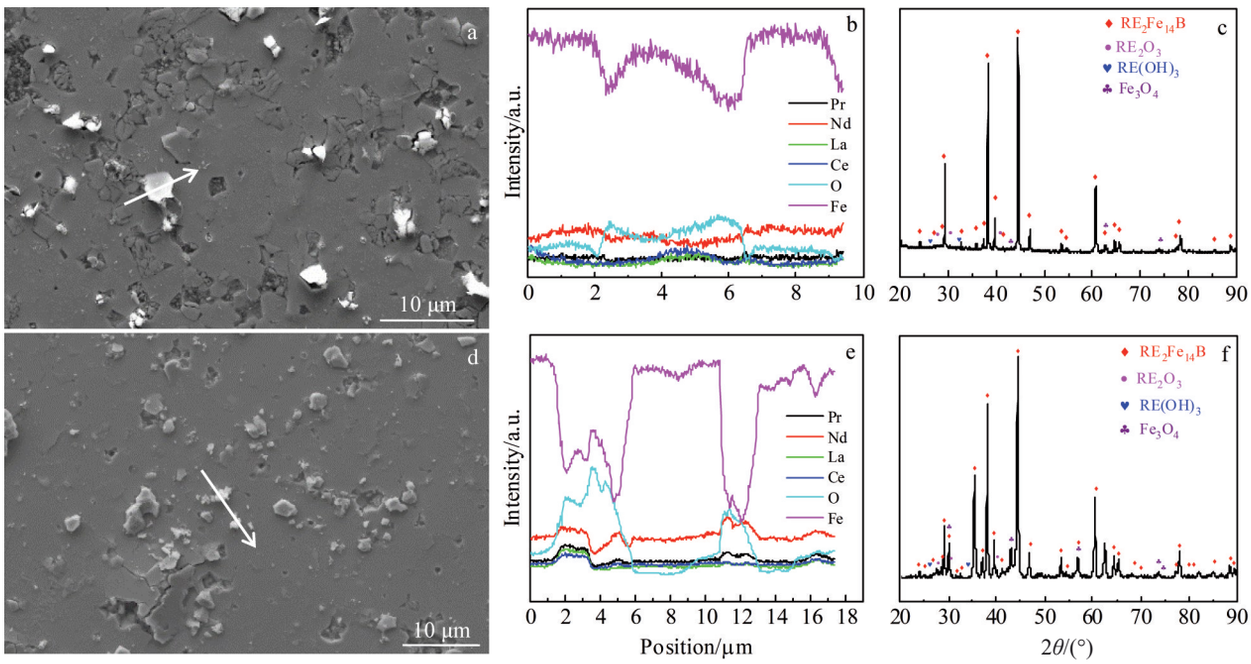

Fig.6 Surface morphologies (a, d), EDS line scanning results along the arrows marked in Fig.6a (b) and 6d (e) and XRD patterns of the cross section vertical to *c*-axis (c, f) for x=0.3 DMP (a–c) and SMP (d–f) magnets exposed under 120 °C, 0.2 MPa and 100% relative humid atmosphere

oxygen and vapor, heterogeneous REs distribution within the individual main grain makes stress appear between LaCe-rich and LaCe-lean regions, further making main phase grain to crush into powders (Fig. 5d and Fig. 6a). In Fig. 6b, Fe is enriched.

3 Conclusions

1) The comparison of magnetic properties and corrosion resistance of $[(Pr, Nd)_{1-x}MM_x]_{30.3}(Fe, Co)_{bal}M_{0.73}B_{0.98}$ (x=0, 0.3, 0.5, 0.7, 1.0, wt%) magnets prepared by double main phase (DMP) and single main phase (SMP) processes with the same MM substitution was implemented. The magnets prepared by the DMP method exhibit much better magnetic properties and corrosion resistance than those by the SMP method.

2) For x=0.5, the magnetic properties of DMP magnets are B_r=1.308 T, H_{cj}=799.98 kA/m, and $(BH)_{max}$=325.6436 kJ/m^3, which are higher than those of SMP magnets (B_r=1.297 T, H_{cj}= 746.8868 kA/m, and $(BH)_{max}$=317.8428 kJ/m^3).

3) Superior corrosion resistance for DMP magnets compared with that of SMP magnets is displayed by mass loss in a hygrothermal environment and electric polarization tests in 3.5wt% NaCl solution. The enhanced RE-rich phase distribution decreases corrosion channels.

4) Due to heterogeneous REs distribution both within one individual grain and across grains for DMP magnets, the stress difference of hydrogen reaction between LaCe-rich and LaCe-lean regions leads to crush of main phase grains under humid and high-temperature atmosphere. That is distinct from the corrosion behavior of SMP magnets. But preferential RE-rich phase corrosion makes main phase grains shed from the bulk magnet for SMP magnets with the same nominal composition.

References

1 Sagawa M, Fujimura S, Togawa N *et al. Journal of Applied Physics*[J], 1984, 55(6): 2083

2 Hu Ba P, Niu E, Zhao Y G *et al. AIP Advances*[J], 2013, 3: 042136

3 Li Ba, Wang Chengbiao, Wang Xiangdong. *Rare Metal Materials and Engineering*[J], 2015, 44(1): 174 (in Chinese)

4 Zhu M G, Han R, Li W *et al. IEEE Transactions on Magnetics*[J], 2015, 51(11): 2104604

5 Zhang M, Liu Y, Li Z B *et al. Journal of Alloys and Compounds*[J], 2016, 688: 1053

6 Zuo W L, Zuo S L, Li R *et al. Journal of Alloys and Compounds*[J], 2017, 695: 1786

7 Jin J Y, Wang Z, Bai G H *et al. Journal of Alloys and Compounds*[J], 2018, 749: 580

8 Hirosawa S, Matsuura Y, Yamamoto H *et al. Journal of Applied Physics*[J], 1986, 59(3): 873

9 Herbst J F. *Review of Modern Physics*[J], 1991, 63(4): 819

10 Stadelmaier H H, Liu N C, Elmasry N A. *Materials Letters*[J], 1985, 3(3): 130

11 Yan C J, Guo S, Chen R J *et al. IEEE Transactions on Magnetics*[J], 2014, 50(10): 2102605

12 Zhang Xuefeng, Shi Yao, Ma Qiang *et al. Rare Metal Materials and Engineering*[J], 2015, 44(3): 748 (in Chinese)

13 Liao X F, Zhao L Z, Zhang J S *et al. Journal of Magnetism & Magnetic Materials*[J], 2018, 464: 31

14 Niu E, Chen Z A, Chen G A *et al. Journal of Applied Physics*[J], 2014, 115(11): 113912

15 Zhu M G, Han R, Li W *et al. IEEE Transactions on Magnetics*[J], 2015, 51(11): 1

16 Jin J Y, Ma T Y, Zhang Y J *et al. Scientific Reports*[J], 2016, 6: 32200

17 Shang R X, Xiong J F, Liu D *et al. Chinese Physics B*[J], 2017, 26(5): 367

18 Zhang Y J, Ma T Y, Jin J Y *et al. Acta Materialia*[J], 2017, 128: 22

19 Jin J Y, Bai G H, Zhang Z H *et al. Journal of Alloys and Compounds*[J], 2018, 763: 854

20 Shang R X, Xiong J F, Liu D *et al. Chinese Physics B*[J], 2017, 26(5): 057502

21 Liu Y L, Ma Q, Wang X *et al. Chinese Physics B*[J], 2020, 29(10): 107504

22 Jin J Y, Yan M, Ma TY *et al. Materials & Design*[J], 2020, 186: 108308

23 Xu J L, Huang Z X, Luo J M *et al. Rare Metal Materials and Engineering*[J], 2015, 44(4): 786

24 Assis O, Sinka V, Ferrante M *et al. Journal of Alloys and Compounds*[J], 1995, 218(2): 263

25 Liu W Q, Yue M, Zhang D T *et al. Journal of Applied Physics*[J], 2009, 105(7): 709

26 Li J J, Li A H, Zhu M G *et al. Journal of Applied Physics*[J], 2011, 109(7): 744

27 Gurrappa I, Pandian S. *Corrosion Engineering Science and Technology*[J], 2006, 41(1): 57

28 Yan G L, Mcguiness P J, Farr J P G *et al. Journal of Alloys and Compounds*[J], 2009, 478(1–2): 188

29 Wu Yaping, Zhu Minggang, Shi Xiaoning *et al. Journal of the Chinese Society of Rare Earths*[J], 2016, 34(2): 171 (in Chinese)

30 Jin J Y, Ma T Y, Yan M *et al. Journal of Alloys and Compounds*[J], 2018, 735: 2225

31 Shi X N, Zhu M G, Zhou D *et al. Journal of Rare Earths*[J], 2019, 37(3): 287

32 Chen F G, Han H C, Zhang T Q *et al. Journal of Magnetism and Magnetic Materials*[J], 2022, 557: 6

33 Jin J Y, Tao Y M, Wang X H *et al. Journal of Materials Science & Technology*[J], 2022, 110: 239

34 Peng B, Jin J, Liu Y *et al. Corrosion Science*[J], 2020, 177

35 Shi X N, Zhu M G, Wang X D *et al. Journal of Rare Earths*[J], 2020, 38(7): 735

36 Wang Jing. *The Research on Magnetic Properties and Microstructure of (PrNd, MM) -Fe-B Stripe Casting Alloys and the Corrosion of the Magnets*[D]. Baotou: Inner Mongolia University of Science and Technology, 2018 (in Chinese)

37 Huang W H, Gao W M, Zuo S W *et al*. *Journal of Materials Chemistry A*[J], 2022, 10: 1290

38 Hu Boping, Rao Xiaolei, Wang Yizhong. *Rare-Earth Permanent Magnet Materials*[M]. Beijing: Metallurgical Industry Press, 2017 (in Chinese)

双主相混合稀土基RE-Fe-B磁体的磁性能和抗腐蚀性改进

连昕丽[1]，周建军[1,3]，李仕林[1]，赵院红[1]，王长鹏[1]，王　印[1]，刘　飞[1]，章　明[1]，左建华[1]，白　锁[1]，刘艳丽[1]，李柱柏[2]，李永峰[1]

(1. 内蒙古科技大学 理学院，内蒙古 包头 014010)

(2. 内蒙古科技大学 材料与冶金学院，内蒙古 包头 014010)

(3. 中科院赣江创新研究院，江西 赣州 341000)

摘　要：为了实现稀土资源的平衡应用且降低RE-Fe-B稀土永磁材料的价格，针对混合稀土基永磁材料进行研究，分别采用单、双主相工艺制备了名义成分$[(Pr,Nd)_{1-x}MM_x]_{30.3}(Fe,Co)_{bal}M_{0.73}B_{0.98}$（$x$=0.3，0.5和0.7，质量分数）的磁体，对比研究其磁性能和抗腐蚀性。研究发现：双主相工艺制备的磁体相比单主相工艺制备的同成分磁体展现了优越的磁性能和抗腐蚀性。当x=0.5，双主相磁体的磁性能为B_r=1.308 T，H_{cj}=799.98 kA/m和$(BH)_{max}$=325.6436 kJ/m^3，远高于同成分的单主相磁体的性能（B_r=1.297 T，H_{cj}=746.8868 kA/m和$(BH)_{max}$=317.8428 kJ/m^3）。这种改进源于富稀土相分布的改进以及主相晶粒间和晶粒内部耦合作用的增强。当双主相磁体暴露在湿热环境下时，磁体中不仅存在富稀土相腐蚀，也存在主相晶粒的腐蚀成粉现象，这主要是由于富稀土相与水蒸气和氧气反应时产生氢气，导致主相晶粒被氢化，由于主相晶粒间和晶粒内部的镧铈分布差异，产生大的应力，导致其表现出区别于单主相磁体的腐蚀行为。

关键词：混合稀土；双主相工艺；磁性能；抗腐蚀性；稀土的非均匀分布

作者简介：连昕丽，女，1996年生，硕士，内蒙古科技大学理学院，内蒙古 包头 014010，E-mail：1612637090@qq.com